Interplay between biquadratic coupling and the Néel transition in $Fe/Cr_{94}Fe_6(001)$ superlattices

Eric E. Fullerton,* C. H. Sowers, and S. D. Bader
Materials Science Division, Argonne National Laboratory, Argonne, Illinois 60439
(Received 14 April 1997)

The commensurate antiferromagnetic order of $Cr_{94}Fe_6$ alloy layers in epitaxial $Fe/Cr_{94}Fe_6(001)$ superlattices was investigated by transport and magnetization techniques. Néel temperature T_N values are strongly thickness dependent, with T_N suppressed for $Cr_{94}Fe_6$ thicknesses < 36 Å. Transport results indicate a broadening of the transition with an onset temperature $T_0 > T_N$ by ≈150 K for all samples. The biquadratic interlayer coupling of the Fe layers is enhanced for $T_N < T < T_0$ and suppressed below T_N. T_0 and T_N are identified with the onset on cooling of inhomogeneous and homogeneous order, respectively, within the spacer layers. The regime of inhomogeneous ordering of the spacer is believed to promote biquadratic coupling because of the dominance of interfacial exchange energies. [S0163-1829(97)08634-7]

I. INTRODUCTION

The interplay between interlayer magnetic coupling and antiferromagnetic (AF) ordering of Cr spacer layers in Fe/Cr superlattices provides interesting insights into the physics of coupled magnetic superlattices. Bulk Cr is an itinerant AF that forms an incommensurate spin-density wave (SDW) below its Néel temperature of $T_N = 311$ K.[1] Previous results on Fe/Cr(001) superlattices[2–4] indicate that the AF incommensurate SDW ordering persists for Cr thicknesses $t_{Cr} > 45$ Å. This raises interesting questions on the role of spin frustration at rough ferromagnetic (F)-AF interfaces. The biquadratic (90°) interlayer coupling observed in Fe/Cr superlattices is directly related to the SDW order of the Cr spacer layer. Biquadratic coupling exists for thin Cr layers (<45 Å), and is strongly temperature dependent increasing monotonically with decreasing temperature. However, for thick Cr layers, biquadratic coupling is only observed for $T > T_N$; it vanishes for $T \leqslant T_N$ upon formation of the SDW.[2,3,5]

In the present work we further explore the role of the Cr ordering by doping the Cr spacer layer with ≈6 at. % Fe to alter the magnetic ordering with the Cr layers as well as the coupling between the Fe layers. We find a temperature window of ≈150 K above T_N for which biquadratic coupling is enhanced that we attributed to inhomogeneous ordering of the spacer. By inhomogeneous ordering, we mean that the AF layer is dominated by the interfacial exchange energies resulting in lateral AF domain sizes being limited by the interfacial terrace widths. Homogeneous ordering refers to AF domains that are large compared to the lateral length scales of the interfacial roughness.

Bulk Cr-Fe alloys have been studied extensively.[6] Fe impurities reduce T_N up to 16 at. % where AF order is suppressed and a spin glass is formed. The incommensurate SDW (AF_1) phase persists up to concentrations of ≈2.5 at. % Fe and then is replaced by commensurate AF_0 order. Therefore, in the present study we investigate coupling without the additional complication of SDW order. The Néel transition in Cr-Fe alloys is first order with a measured latent heat of 5 J/mole for 6 at. % Fe.[7] Both neutron scattering and susceptibility results indicate that the Cr AF state coexists with magnetic moments localized at the Fe sites.[6,8] The temperature dependence of the magnetic susceptibility exhibits a Curie-Weiss behavior both above and below T_N, with a Curie-Weiss temperature θ of 10–30 K and a local Fe moment of $\approx 3\mu_B$ for Fe concentrations near 6 at. %. The residual resistance increases linearly with Fe at a rate of ≈7 $\mu\Omega$ cm per at. % Fe. In addition, the resistance anomaly below T_N in Cr-Fe alloys is enhanced over that observed for Cr and other Cr alloys. We exploit the resistance anomaly as a probe of the AF ordering process in order to monitor the influence of ordering on the interlayer coupling.

The interlayer coupling in Fe/Cr/Fe(001) structures is characterized by the phenomenological energy expression $E = J_1(\mathbf{m}_1 \cdot \mathbf{m}_2) + J_2(\mathbf{m}_1 \cdot \mathbf{m}_2)^2$ where J_1 and J_2 are the bilinear and biquadratic exchange-coupling terms and $\mathbf{m}_1$, $\mathbf{m}_2$ are the magnetization of two adjacent Fe layers.[9,10] J_1 oscillates in sign with increasing Cr thickness resulting in either F or AF alignment of adjacent magnetic layers. In Fe/Cr/Fe(001) structures, two oscillatory periods have been observed: a short, 2.1-monolayer (ML) period in samples with atomically smooth Cr interfaces,[11] and a long, 18-Å period which is independent of crystallographic orientation.[12] These periods are governed by spanning vectors that join extremal points of the Fermi surface normal to the layering direction.[13] The short-period oscillation is universally accepted to result from the nested feature in the ⟨100⟩ direction of the Cr Fermi surface which also is responsible for the SDW AF of Cr. The isotropic long period, while still a topic of active debate, is understood to originate from a short spanning-vector associated with either the ''lens'' or the N-centered ellipse feature of the Fermi surface.[14–17]

The biquadratic coupling term is found to be nonoscillatory and favors 90° alignment of adjacent Fe layers. The origin of the biquadratic coupling is less well understood than the bilinear coupling. Slonczewski[10] proposed two mechanisms: fluctuations in the spacer thickness which averages over a short-period oscillation, and superparamagnetic impurities (''loose spins'') within the spacer. The first mechanism was developed for Fe/Cr(001) because of the prominent short-period coupling observed in this system.[18] The mechanism assumes that the Cr layer can be described by terraces separated by monoatomic steps. The coupling across each terrace region will be F or AF and will alternate

from one neighboring terrace to the next. If the terrace widths are small compared to an Fe domain, the energy of the system is lowered by perpendicular alignment of the entire Fe layer magnetization with respect to that of the adjacent Fe layer. Shender and Holdsworth[19] have generalized this problem to remove the restrictions on the form of the terraces and find that the biquadratic coupling depends on the effective dimension of the disorder.

The fluctuation model was modified to include the intrinsic AF ordering of Cr or Mn spacers, and is referred to as a proximity magnetism model. The form of the energy expression describing the 90° coupling is given by

$$E(\Delta\theta)=\frac{J_2}{\pi^2}[(\Delta\theta)^2+(\Delta\theta-\pi)^2], \tag{1}$$

where $\Delta\theta$ is the relative angle between adjacent magnetic layers. This coupling arises from inhomogeneous ordering of the AF interlayers in which a spiral structure is formed within a terrace which rotates with opposite sense of rotation in neighboring terraces. This model was successfully used to explain the magnetism of the CoFe/Mn superlattices.[20] The applicability of this model to the Fe/Cr system is not established and will depend on the magnetic ordering of the Cr in the presence of a stepped or rough interface.

Experiments on epitaxially sputtered Fe/Cr(001) superlattices found the incommensurate Néel transition of the Cr spacers observed in transport methods vanishes for Cr thicknesses $t_{Cr}<45$ Å.[2] For $t_{Cr}>45$ Å for Cr, T_N increases rapidly and asymptotically approaches the bulk value for thick Cr spacers. For $t_{Cr}\geqslant 51$ Å, neutron scattering finds a transverse SDW (AF_1) is formed with a single Q normal to the layers and the nodes of the SDW near the Fe-Cr interfaces.[3] For the $t_{Cr}=31$ Å and 44 Å, the magnetic scattering is described by AF_0 ordering without clear evidence of an incommensurate Néel transition in magnetization or transport studies. The crossover from commensurate to AF_1 SDW order with increasing Cr thickness was first observed by Ungurus, Celotta, and Pierce[11,21] for Cr films on an Fe whisker by means of magnetic imaging experiments. This crossover has also recently been observed by Schreyer *et al.*[4] by means of neutron scattering from Fe/Cr(001) superlattices grown by molecular beam epitaxy. This behavior is understood theoretically as arising from a critical thickness needed to support SDW order.[22]

II. EXPERIMENTAL PROCEDURE

The (001)-oriented $Cr_{94}Fe_6$ films and Fe/$Cr_{94}Fe_6$ superlattices were grown by dc magnetron sputtering onto epitaxially polished single-crystal MgO(100) substrates. The $Cr_{94}Fe_6$ layers are deposited by co-sputtering from elemental sources using the relative deposition rates of the sources to adjust the composition. A 100 Å-Cr buffer layer was initially deposited at a substrate temperature T_S of 600 °C to establish the epitaxial orientation with the substrate.[12] The substrate was then cooled to 150–500 °C to grow the $Cr_{94}Fe_6$ films and 150 °C to grow superlattices with 15-Å Fe layers and Cr-Fe layers varying from 8–440 Å. Thin Fe layers were chosen to minimize the current carried by the Fe layers in the transport measurements. The structures were characterized by x-ray diffraction using Cu-K_α radiation. Shown in Fig. 1 are x-ray diffraction results for an [Fe(15 Å)/$Cr_{94}Fe_6$(46 Å)]$_{40}$ superlattice. The x-ray scan confirms the (001) growth with a 0.7° mosaic spread, as indicated by the full width at half maximum of the rocking curve scan of the (002) reflection (shown in the inset of Fig. 1). Also, superlattices peaks are observed about the (002) reflection indicating a well-defined superlattice structure. Magnetic properties were measured by superconducting quantum interference device magnetometry equipped with both longitudinal and transverse coils. Mangeto-transport was measured by means of a standard four-probe technique in a Quantum Design Physical Properties Measurement System in fields up to 9 T.

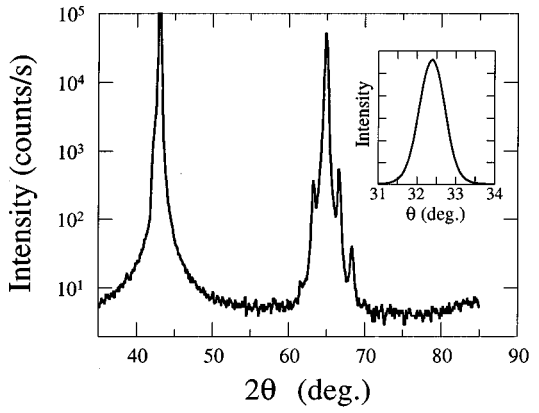

FIG. 1. X-ray diffraction results for an [Fe(15 Å)/$Cr_{94}Fe_6$ (46 Å)]$_{40}$ superlattice grown on MgO(100). The inset shows the rocking curve scan of the main superlattice reflection (2θ=64.87°).

III. NÉEL TRANSITION

Shown in Fig. 2 are transport results for a 2000-Å thick

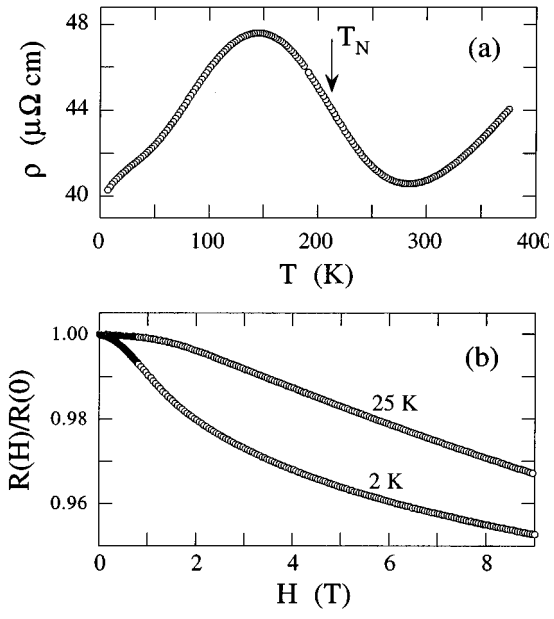

FIG. 2. Transport results for a 2000-Å thick $Cr_{94}Fe_6$ alloy film grown at T_S=500 °C. (a) ρ vs T. The arrow indicates T_N determined from the minimum of $d\rho/dT$ vs T. (b) Magnetoresistance measured at 2 and 25 K.

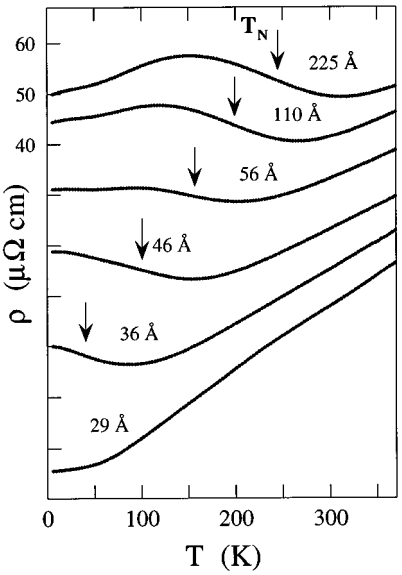

FIG. 3. Resistivity results for a series of $[Fe(15\ Å)/Cr_{94}Fe_6(t_{Cr\text{-}Fe})]_{40}$ superlattices. The $t_{Cr\text{-}Fe}$ values are shown. The resistivity scale is for the 225-Å sample. The scale is offset 10, 15, 30, 45, and 50 $\mu\Omega$ cm for subsequent samples. The arrows indicate T_N determined from the minimum of $d\rho/dT$ vs T, as shown in Fig. 4.

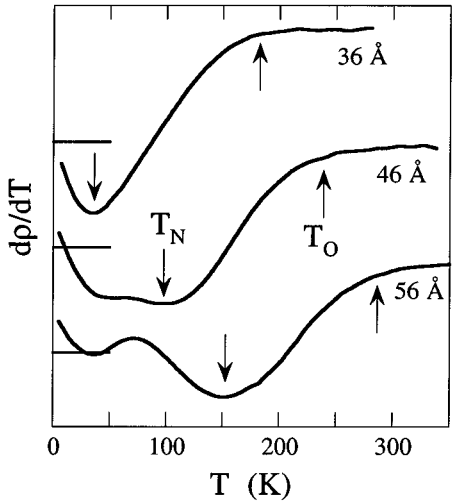

FIG. 4. $d\rho/dT$ vs T for the 36-, 46-, and 56-Å samples of Fig. 3. The arrows indicate T_N and the onset temperature T_0 where the resistivity deviates from a linear T dependence. The curves are offset for clarity and the horizontal lines indicate $d\rho/dT=0$ for each sample.

$Cr_{94}Fe_6$ film grown at $T_S=500$ °C. The characteristic increase in resistivity ρ below T_N is evident in Fig. 2(a). T_N is determined operationally from the point of inflection of the ρ vs T (i.e., the minimum in $d\rho/dT$). Using this criterion, we obtain $T_N=212\pm5$ K which agrees with $T_N=211$ K obtained for a bulk Cr-Fe alloy with 6.5 at. % Fe.[6] The relatively high residual resistivity of the film in Fig. 2(a) as compared to pure Cr films also agrees with bulk results. The transition, however, is considerable broader and does not exhibit the first-order jump in ρ observed in bulk crystals. This difference may result from a nonuniform Fe distribution or clustering in the alloy arising from nonequilibrium thin-film growth. For $Cr_{94}Fe_6$ films grown at lower T_S (=150 °C), T_N increases to ≈260 K which again may result from differences in the Fe distribution. Shown in Fig. 2(b) is the magnetoresistance (MR) measured at 2 and 25 K. The MR is large and negative. Both the magnitude and shape of the MR curve agree with bulk measurements and are characteristic of magnetic alloys.[8] The presence of local moments provides spin-flip scattering channels which are frozen out in high magnetic fields.

Shown in Fig. 3 are the resistivity curves for a series of Fe(15 Å)/$Cr_{94}Fe_6$ superlattices. For thicker Cr-Fe layers (e.g., 225 Å) the resistivity curve is similar to the Cr-Fe film results of Fig. 2. As the Cr-Fe layer thickness is reduced, the minimum in ρ vs T as well as the inflection point characterizing T_N (indicated by the arrows), shifts to lower temperatures. T_N decreases systematically with decreasing Cr-Fe spacer thickness in a qualitatively similar fashion to that observed for Fe/Cr superlattices.[3] For the 29-Å Cr-Fe spacer, the resistivity decreases monotonically with decreasing temperature without showing the upturn characteristic of the Néel transition in Cr-Fe alloys. These results suggest a suppression of the homogeneous ordering for Cr-Fe spacer layers less than ≈33 Å. Shown in Fig. 4 is $d\rho/dT$ for the 36-, 46-, and 56-Å Cr-Fe spacers. From the $d\rho/dT$ curves, we extract two temperatures: T_N determined by the minimum in $d\rho/dT$ and the onset temperature T_0, which we define as the temperature at which the resistivity deviates from its linear ρ vs T behavior. This definition of T_N was previously shown to agree with neutron diffraction results in Fe/Cr superlattices.[3] For all the samples studied, T_0 was ≈150 K higher than T_N.

IV. MAGNETIZATION AND MAGNETORESISTANCE

Shown in Fig. 5 are the magnetotransport results for samples shown in Fig. 4 measured at $T>T_0$, $T_N<T<T_0$, and $T<T_N$. For $T>T_0$ the MR is small and positive for small fields. (The negative high-field MR has been subtracted from the data.) This positive MR results from the anisotropic magnetoresistance (AMR) as the Fe layers rotate from the Fe[100] easy-axis direction to saturated along the [110]. This shows that the Fe layers are either uncoupled or ferromagnetically coupled in this temperature range with the saturation field proportional to the cubic anisotropy. For $T_N<T<T_0$ the MR behavior becomes negative and isotropic and is characteristic of the giant magnetoresistance (GMR), and the saturation field increases. As temperature decreases to $T<T_N$, the MR changes sign back to that for AMR behavior for the 46- and 56-Å samples and is strongly reduced for the 36-Å sample. For the 29-Å sample, the MR is negative and decreased monotonically with increasing T. These results are summarized in Fig. 6, showing the T dependence of the MR. For $t_{Cr\text{-}Fe}\geq36$ Å, GMR is only observed in the intermediate temperature range $T_N<T<T_0$ as indicated by the arrows. This change in behavior is also observed in the magnetic behavior. Shown in Fig. 7 are magnetization results for the 36-Å sample. For $T>T_0$, a square hysteresis loop is observed consistent with the AMR behavior observed in Fig. 5. For $T<T_0$, the remanent magnetization decreases indicat-

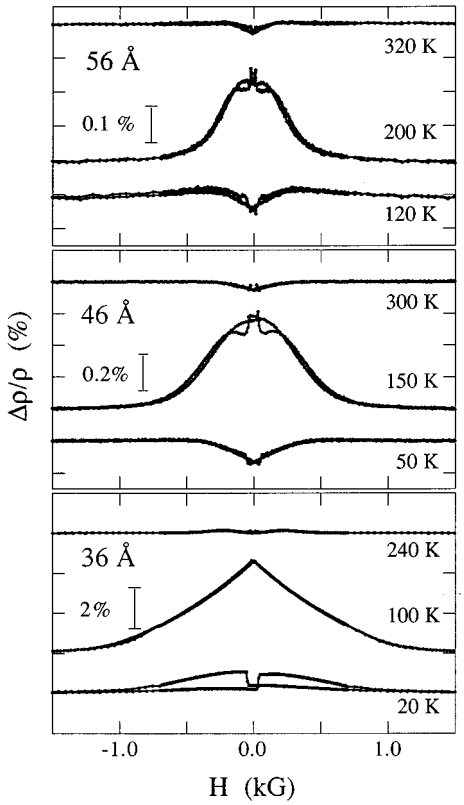

FIG. 5. Low-field magnetoresistance curves for the samples shown in Fig. 4. Top panel (56-Å spacer layer), middle panel (46 Å), and bottom panel (36 Å). H is parallel to the current and parallel to the Fe[110] hard axis. The linear high-field contribution to the MR has been subtracted from the data. For each panel, the top curve is for $T>T_0$, the middle curve $T_0>T>T_N$, and the bottom curve $T<T_N$.

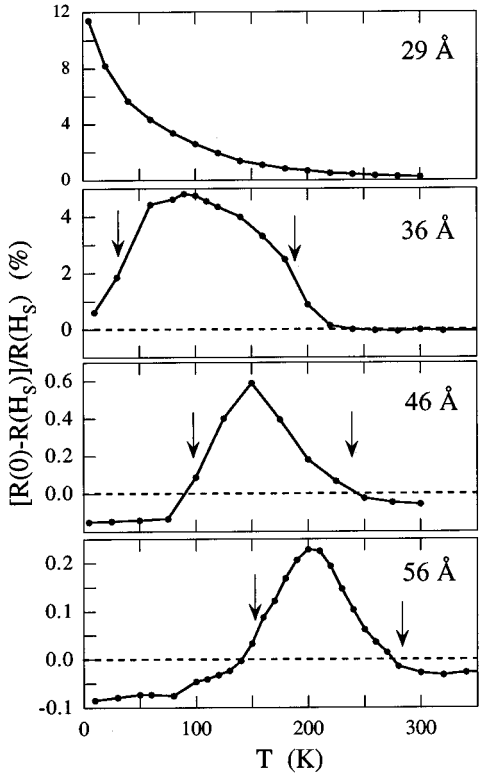

FIG. 6. Magnetoresistance values vs T for superlattices the 29-, 36-, 46-, and 56-Å samples. $\Delta\rho$ is defined such that $\Delta\rho<0$ is characteristic of AMR behavior and $\Delta\rho>0$ is GMR. The arrows indicate the T_N and T_0 values as determined in Fig. 4.

ing the onset of interlayer coupling. The remanent value of 0.58 and the shape of the hysteresis loop can be quantitatively modeled assuming a combination of ferromagnetic bilinear coupling, biquadratic coupling, and cubic anisotropy. For lower temperatures, a square hysteresis loop is again regained. The temperature dependence of the remnant magnetization is plotted in Fig. 8. We observe the onset of biquadratic coupling below T_0 and then a suppression below T_N. The change in magnetic properties of the magnetic layer is also reflected in the coercive fields, H_C. We find enhanced H_C values below T_N. An example is shown in Fig. 9 for the 46-Å sample.

We only observed AF bilinear coupling for Cr-Fe thicknesses of ≈8–10 Å which corresponds to the first AF-coupling maximum for Cr spacers. We did not observe the oscillatory coupling for thicker Cr-Fe spacers previously observed for Cr.[12] This most likely results from the high resistance of the Cr-Fe alloy compared to that of Cr spacers. Therefore, we could not study the interaction between T_N and the bilinear coupling in the present samples.

V. DISCUSSION AND CONCLUSION

These results again highlight the direct relationship between the intrinsic AF order of the spacer layer and the biquadratic interlayer coupling. The Néel transition measured via transport is found to decrease with decreasing Cr thickness in a qualitatively similar fashion to that previously reported for Fe/Cr superlattices. This behavior is understood as arising from frustration caused by interfacial roughness.[2] For thin layers, the Cr layers are coupled to the Fe layers and will order locally (i.e., within the lateral terrace length) as shown schematically in Fig. 10(a). Such a configuration is obtained in calculations of F/AF systems with rough interfaces.[23–25] As the spacer layer thickness increases, this configuration is unstable and will crossover to homogeneous ordering shown schematically in Fig. 10(b). In this configuration, the disorder is located near the interface and the center of layer exhibits long-range order. A transition from homogeneous ordering to inhomogeneous ordering is also expected with increasing temperature.[23] For temperatures in the vicinity of T_N, the ordering of the spacer layer is dominated by the interfacial exchange energy and will locally respond to the Fe layers. For thicker spacer layers and low temperatures, the intrinsic AF ordering of the spacer should dominate and homogeneous AF ordering is expected [Fig. 10(b)]. For small spacer thicknesses or T near T_N, inhomogeneous ordering is expected.

Within either the fluctuation or proximity magnetism models the existence of biquadratic coupling implies inhomogeneous ordering of the Cr or Cr-Fe interlayers. That is, the AF interlayer has to respond to local fluctuations at the interface. Therefore, biquadratic coupling is expected for a magnetic configuration shown in Fig. 10(a). For a homogeneously ordered layer, the magnetism of the Cr layers will be insensitive to the relative orientation of the Fe layers, and

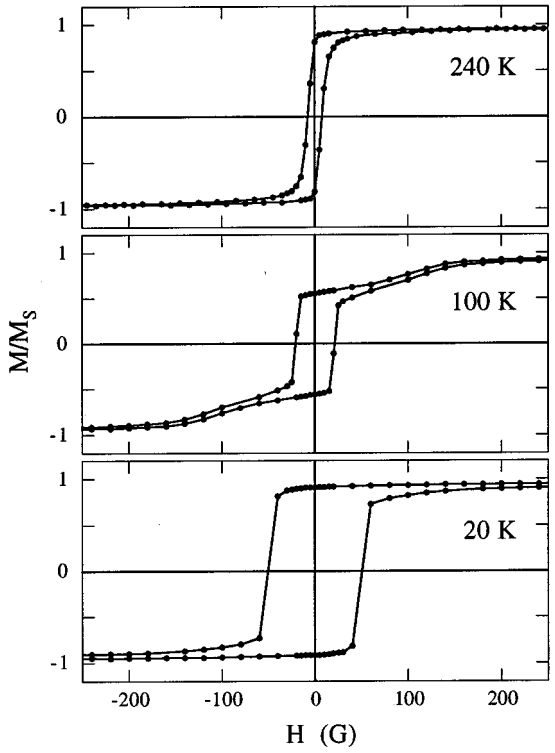

FIG. 7. Magnetic results for the $[\mathrm{Fe}(15\ \text{Å})/\mathrm{Cr_{94}Fe_6}(36\ \text{Å})]_{40}$ superlattice with H applied along the Fe[100] easy axis. The top panel is for $T>T_0$, the middle panel $T_0>T>T_N$, and the bottom panel $T<T_N$.

thus the biquadratic coupling should be suppressed. There may still be an effect on the coercive field as observed for thin Fe layers on a Cr substrate.[26] Thus to interpret the present results, the onset temperature T_0 is the boundary between the paramagnetic spacer and inhomogeneous ordering. In the fluctuation model, the Cr-Fe interlayer would be viewed as having an enhanced susceptibility as T approaches T_N, whereas the proximity magnetic model assumes inhomogeneous AF order. T_N then denotes the transition to homogeneous order, and is concomitant with the suppression of

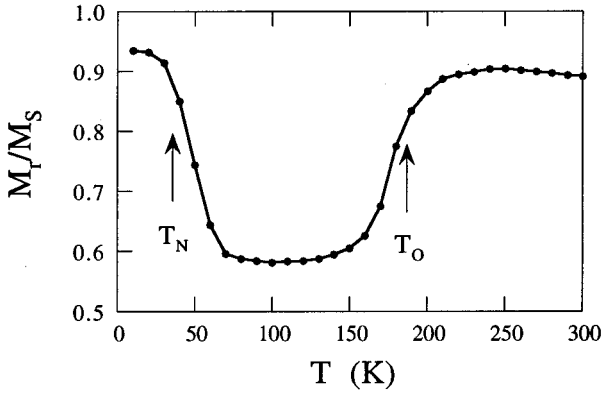

FIG. 8. Remanent magnetization M_r/M_s values for the $[\mathrm{Fe}(15\ \text{Å})/\mathrm{Cr_{94}Fe_6}(36\ \text{Å})]_{40}$ superlattice with H applied along the Fe[100] easy axis. Arrows indicate T_N and T_0 values determined in Fig. 4.

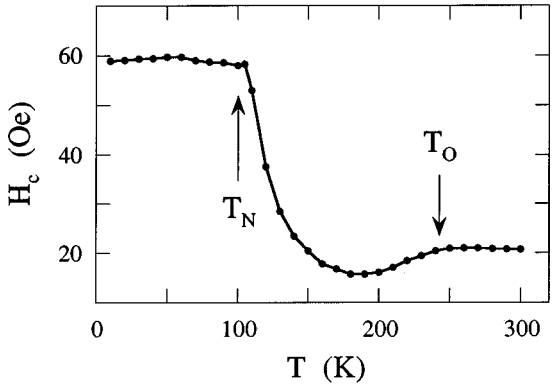

FIG. 9. Coercive field H_C values for the $[\mathrm{Fe}(15\ \text{Å})/\mathrm{Cr_{94}Fe_6}(46\ \text{Å})]_{40}$ superlattice with H applied along the Fe[100] easy axis. Arrows indicate T_N and T_0 values determined in Fig. 4.

biquadratic coupling. For the thinnest Cr-Fe layers, the homogeneous ordering is never achieved and the biquadratic coupling increases monotonically with decreasing temperature. This interpretation is consistent with Ref. 4 which correlated the presence of biquadratic coupling in Fe/Cr(001) superlattices with the observation, via neutron scattering, of frustrated AF_0 order.

In conclusion, we have investigated the AF ordering of $\mathrm{Cr_{94}Fe_6}$ alloy layers in epitaxial $\mathrm{Fe/Cr_{94}Fe_6}(001)$ superlattices. Néel temperature T_N values are found to be strongly

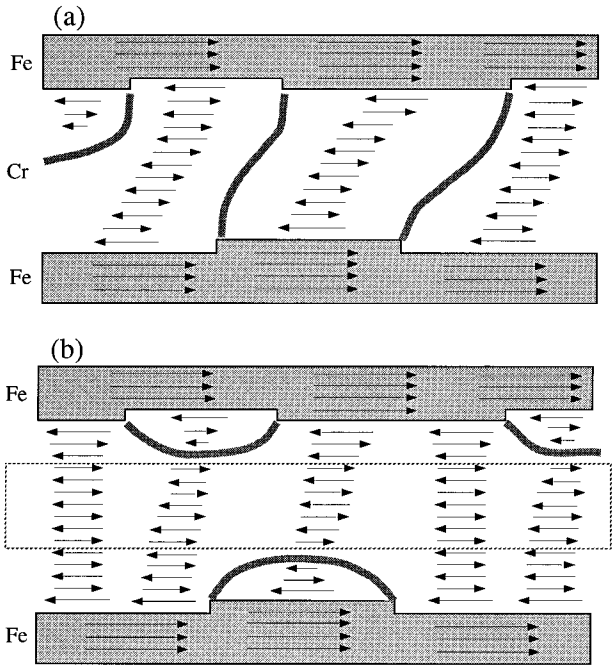

FIG. 10. Schematic representation of two possible magnetic ordering configurations for an AF spacer layer in the presence of rough interfaces. In both cases, domain walls (indicated by broad lines) are initiated and terminated at interfacial steps. (a) Domain walls connect steps at adjacent Fe layers resulting in inhomogeneous ordering of the AF spacer layer and (b) domain walls connect steps of the same Fe layers resulting in homogeneous ordering within the center of the AF layer indicated by the dashed line.

thickness dependent, with T_N suppressed for $Cr_{94}Fe_6$ thicknesses less than ≈33 Å. Transport results indicate a broadening of the transition with an onset temperature $T_0 > T_N$ by ≈150 K for all thicknesses. The biquadratic interlayer coupling of the Fe layers is enhanced between T_N and T_0 and suppressed below T_N. These results show a direct correlation between the AF ordering process and the biquadratic interlayer coupling.

ACKNOWLEDGMENT

Work supported by the U.S. DOE, BES-Materials Sciences, under Contract No. W-31-109-ENG-38.

*Present address: IBM Almaden Research Center, Mailstop K63/803, 650 Harry Rd., San Jose, CA 95120-6099.

[1] E. Fawcett, Rev. Mod. Phys. **60**, 209 (1988).

[2] E. E. Fullerton, K. T. Riggs, C. H. Sowers, S. D. Bader, and A. Berger, Phys. Rev. Lett. **75**, 330 (1995).

[3] E. E. Fullerton, S. D. Bader, and J. L. Robertson, Phys. Rev. Lett. **77**, 1382 (1996).

[4] A. Schreyer, C. F. Majkrzak, T. Zeidler, T. Schmitte, P. Bödeker, K. Theis-Bröhl, A. Abromeit, J. Dura, and T. Watanabe (unpublished).

[5] J. F. Ankner, H. Kaiser, A. Schreyer, T. Zeidler, H. Zabel, M. Schäfer, and P. Grünberg, J. Appl. Phys. (to be published).

[6] E. Fawcett, H. L. Alberts, V.Y. Galkin, D. R. Noakes, and J. V. Yakhmi, Rev. Mod. Phys. **66**, 25 (1994).

[7] L. G. Maystrenko and V. M. Polovov, Phys. Met. Metallogr. **43**, 79 (1977).

[8] F. T. Hedgcock, J. O. Strom-Olsen, and D. F. Wilford, J. Phys. F **7**, 855 (1977).

[9] B. Heinrich and J. F. Cochran, Adv. Phys. **42**, 523 (1993).

[10] J. C. Slonczewski, J. Magn. Magn. Mater. **150**, 13 (1995).

[11] J. Unguris, R. J. Celotta, and D. T. Pierce, Phys. Rev. Lett. **67**, 140 (1991).

[12] E. E. Fullerton, M. J. Conover, J. E. Mattson, C. H. Sowers, and S. D. Bader, Phys. Rev. B **48**, 15 755 (1993).

[13] P. Bruno, Phys. Rev. B **52**, 411 (1995).

[14] M. D. Stiles, Phys. Rev. B **48**, 7238 (1993).

[15] D. D. Koelling, Phys. Rev. B **50**, 273 (1994).

[16] M. D. Stiles (unpublished).

[17] D. Li, J. Pearson, S. D. Bader, E. Vescovo, D.-J. Huang, P. D. Johnson, and B. Heinrich, Phys. Rev. Lett. **78**, 1154 (1997).

[18] J. C. Slonczewski, Phys. Rev. Lett. **67**, 3172 (1991).

[19] E. F. Shender and P. C. W. Holdsworth, Phys. Rev. Lett. **76**, 2583 (1996).

[20] M. E. Filipkowski, J. J. Krebs, G. A. Prinz, and C. J. Gutierrez, Phys. Rev. Lett. **75**, 1847 (1995).

[21] J. Unguris, R. J. Celotta, and D. T. Pierce, Phys. Rev. Lett. **69**, 1125 (1992).

[22] Z.-P. Shi and R. S. Fishman, Phys. Rev. Lett. **78**, 1351 (1997).

[23] A. Berger and E. E. Fullerton, J. Magn. Magn. Mater. **165**, 471 (1997).

[24] E. E. Fullerton, K. T. Riggs, C. H. Sowers, A. Berger, and S. D. Bader, in *Magnetic Ultrathin Films, Multilayers and Surfaces*, edited by A. Fert *et al.*, MRS Symposia Proceedings No. 384 (Material Research Society, Pittsburgh, 1995), p. 145.

[25] D. Stoeffler and G. Gautier, J. Magn. Magn. Mater. **156**, 114 (1996).

[26] A. Berger and H. Hopster, Phys. Rev. Lett. **73**, 193 (1994).